

Cite this: *RSC Adv.*, 2018, **8**, 20379

## Preparation of polycarboxylic acid-functionalized silica supported Pt catalysts and their applications in alkene hydrosilylation†

Dongyun Shao and Youxin Li  \*

A series of novel immobilized platinum catalysts was prepared by loading Pt onto silica particles modified with polycarboxylic acid groups such as diethylenetriaminepentaacetic acid (DTPA), nitroltriacetic acid (NTA) and succinic acid (SA). The three modified heterogeneous Pt catalysts were characterized using infrared spectroscopy (IR), transmission electron microscopy (TEM), X-ray photoelectron spectroscopy (XPS), energy dispersive X-ray spectroscopy (EDS) and atomic absorption spectroscopy (AAS). The residual  $H_2PtCl_6$  solutions were characterized using ultraviolet spectroscopy (UV). The polycarboxylic acid-functionalized silica supported Pt catalysts were used to catalyze alkene hydrosilylation and 1-hexene was chosen as a model alkene. The data indicated that the catalytic performance was strongly dependent on the properties of the polycarboxylic acid group bonded to the silica particles. Among them, DTPA-functionalized silica supported Pt ( $SiO_2$ -DTPA-Pt) showed the best catalytic activity and reusability. Furthermore, some hydrosilylation reactions between other linear alkenes (1-heptene, 1-octene, 1-decene, 1-do-decene, 1-tetra-decene, 1-hexa-decene, 1-octa-decene, styrene or *cis*-hex-2-ene), or ring type alkenes (norbornene) with methylidichlorosilane could be catalyzed in the presence of these three Pt catalysts. Their high activities were more than 90%, and their selectivities were more than 99%, which were apparently better than homogeneous Pt catalysts. In addition, reactions with cyclohexene were also successfully catalyzed by the Pt catalysts. These results indicate that the polycarboxylic acid-functionalized silica gel supported Pt catalysts have potential value in industrial hydrosilylation reactions.

Received 1st March 2018  
Accepted 18th May 2018

DOI: 10.1039/c8ra01828f

[rsc.li/rsc-advances](http://rsc.li/rsc-advances)

## 1 Introduction

Platinum catalysts have received much attention from many researchers because of their significant applications in many fields. They can be used to catalyze the hydrosilylation reaction of olefins since Speier *et al.*<sup>1</sup> discovered that hexachloroplatinic acid was a very active catalyst for hydrosilylation reactions. Besides, some varieties of Pt catalyst can also be used to catalyze  $NO_x$  reduction by hydrogen,<sup>2,3</sup> hydrogenation processes,<sup>4,5</sup> the oxidation of alcohols,<sup>6</sup> dehydrogenation reactions<sup>7</sup> and so forth. Among these reactions, the hydrosilylation of alkenes is a crucial reaction on both the industrial and laboratory scale. It is a carbon–silicon bond forming reaction, providing access to organofunctional silanes and silicones, which are commonly used for the production of cross-linkers, adhesives and

polymers.<sup>8,9</sup> Today, hydrosilylation reactions are usually activated by homogeneous catalysts such as Speier's catalyst (hexachloroplatinic acid),<sup>1</sup> Karstedt's catalyst<sup>10</sup> and Markó's catalyst<sup>11</sup> due to their unparalleled catalytic activities. However, these homogeneous Pt catalysts have high cost, poor selectivity<sup>12</sup> and non reusability and result in environmental pollution.<sup>13</sup> Moreover, due to their extremely high reactivity, the catalysts often require an inert atmosphere to play a better role and avoid potential risk, which restricts their utility for large scale industrial production.

The development of heterogeneous catalysts with high activity, selectivity and reusability was necessary and had been studied over the past few decades. Varieties of supported material were used to prepare the heterogeneous Pt catalysts, such as silica,<sup>14,15</sup> mesostructured silica,<sup>16</sup>  $Al_2O_3$ ,<sup>17,18</sup> glass fiber,<sup>19</sup> polystyrene,<sup>20</sup> polyethylene glycol,<sup>21</sup> polyamide,<sup>22</sup> carbon,<sup>23</sup> graphene oxide<sup>24</sup> and titania.<sup>25</sup> Among these materials, silica is a theoretically good support material because it has high mechanical strength and high surface area and it is non-volatile, cheap and non-toxic. Besides, there are a large number of silicon hydroxyl groups on the surface of silica which can be easily modified with varieties of functional group such as

Tianjin Key Laboratory for Modern Drug Delivery and High-Efficiency, Collaborative Innovation Center of Chemical Science and Engineering, School of Pharmaceutical Science and Technology, Tianjin University, Room C412-8, Building 24, 92 Weijin Road, Nankai District, Tianjin 300072, China. E-mail: [lyx@tju.edu.cn](mailto:lyx@tju.edu.cn); Fax: +86-22-2789-2820; Tel: +86-22-2789-2820

† Electronic supplementary information (ESI) available. See DOI: [10.1039/c8ra01828f](https://doi.org/10.1039/c8ra01828f)



sulfonate, phosphate, amine, *etc.*, to increase the stability of the supported catalysts during the catalytic reaction.

polycarboxylic acids such as diethylenetriaminepentaacetic acid (DTPA), ethylenediaminetetraacetic acid (EDTA), nitro-lotriacetic acid (NTA) and succinic acid (SA) are chelating agents and can form very stable chelates with metals.<sup>26</sup> They were proved to efficiently complex to various metals. Almeida *et al.*<sup>27</sup> prepared DTPA functionalized magnetic nanoparticles to separate Nd<sup>3+</sup> and La<sup>3+</sup> and achieved a high separation efficiency (>99%). Shiraishi *et al.*<sup>28</sup> used several inorganic adsorbents (silica gel, MCM-41, and aluminum oxide) modified by EDTA and DTPA as chelating ligands to absorb transition metals such as Cu<sup>2+</sup>, Ni<sup>2+</sup>, VO<sup>2+</sup>, Zn<sup>2+</sup>, Co<sup>2+</sup> and Mn<sup>2+</sup>. Baraka *et al.*<sup>29</sup> synthesized a new chelating resin by anchoring NTA and used it to remove Cu<sup>2+</sup> from synthetic wastewater. Ikodiya *et al.*<sup>30</sup> successfully removed Ca<sup>2+</sup> from synthetic wastewater using SA modified red onion skin extract. Efforts in our laboratory have been directed towards creating EDTA-functionalized silica-supported Pt catalysts.<sup>31</sup> However, DTPA, NTA or SA functionalized silica gel have never been used as the support for Pt immobilization until this paper.

In this paper, to further extend our ongoing efforts towards the development of such polycarboxylic acid-functionalized Pt catalysts and to explore and compare their applications in alkene hydrosilylation, we report herein three novel polycarboxylic acid (including DTPA, NTA and SA)-functionalized silica gel supported Pt catalysts. The characteristics and catalytic ability of the three Pt catalysts were checked. Their catalytic activity and reusability were preliminarily evaluated using 1-hexene hydrosilylation with methylchlorosilane. Their catalytic efficiency and selectivity were further verified through catalyzing these hydrosilylation reactions between methylchlorosilane and a series of linear alkenes (1-heptene, 1-octene, 1-decene, 1-do-decene, 1-tetra-decene, 1-hexa-decene, 1-octa-decene, *cis*-hex-2-ene, styrene) and ring type alkenes (norbornene and cyclohexene).

## 2 Experimental

### 2.1 Materials

All commercially available solvents and reagents were analytical grade or better and were directly used without further purification unless otherwise stated. Silica gel was obtained from Yantai Xinnuo Chemical Industry Co., Ltd. (Shandong, China). Diethylenetriaminepentaacetic acid, nitrolotriacetic acid, 1-hexene (99%), 1-heptene (99%), 1-hexa-decene (95%) and 1-octo-decene (≥95%) were from Shanghai Macklin Biochemical Co., Ltd. (Shanghai, China). Butanedioic anhydride was from Tianjin Guangfu Fine Chemical Research Institute (Tianjin, China). 1-Octene (99%) and norbornene (99%) were from J&K Scientific Ltd. (Beijing, China). 1-Do-decene (95%) and 1-tetra-decene (99%) were from Meryer Chemical Technology Co., Ltd. (Shanghai, China). 1-Decene (≥95%) was from Adamas Reagent Co., Ltd. (Shanghai China). Dichloromethylhexylsilane (98%) was from CNW Technologies Co., Ltd. (Nordrhein Westfalen, Germany). *cis*-2-Hexene was from Alfa Aesar Co., Ltd. (Massachusetts, USA). H<sub>2</sub>PtCl<sub>6</sub>·6H<sub>2</sub>O and cyclohexene (≥98%)

were from Tianjin Kemot Chemical Technology Co., Ltd. (Tianjin, China). CDCl<sub>3</sub> was from Energy Chemical Co., Ltd. (Shanghai, China). Other solvents were obtained from Tianjin Jiangtian Scientific Co., Ltd. (Tianjin, China).

### 2.2 Instruments

The immobilized Pt catalysts and other intermediates were characterized using infrared spectroscopy (IR, TENSOR 27, Bruker, Germany), transmission electron microscopy (TEM, JEM 2100F, JEOL Ltd., Japan), high-resolution transmission electron microscopy (HRTEM, JEM 2100F, JEOL Ltd., Japan), energy dispersive X-ray spectroscopy (EDS, X-Max, Oxford Instruments Ltd., Britain) and X-ray photoelectron spectroscopy (XPS, PHI-1600, PerkinElmer, US). Residual H<sub>2</sub>PtCl<sub>6</sub> solutions were characterized using an ultraviolet-visible spectrophotometer (UV, U-3900, Hitachi, Japan). Pt loading was analyzed using an atomic absorption spectrophotometer (AAS, 180-80, Hitachi, Japan). The hydrosilylation products and diethylenetriaminepentaacetic dianhydride (DTPAD) were identified using a Bruker Advance 600 MHz spectrometer (Bruker, Germany). The quantitative analysis of all hydrosilylation products were analyzed using GC with a capillary column (30 m × 0.25 mm × 0.25 μm) coated with 5% phenyl and 95% methyl polysiloxane.

### 2.3 Synthesis of Pt catalyst loaded on DTPA-functionalized silica gel (SiO<sub>2</sub>-DTPA-Pt)

**2.3.1 Synthesis of DTPAD.** DTPAD was synthesized according to the method reported previously by Tülü *et al.*<sup>32</sup> as shown in Fig. 1(B). Briefly, 23 g (0.06 mmol) DTPA was first dissolved in 30 ml (0.36 mmol) anhydrous pyridine in a 100 ml three-neck round flask with a straight condenser installed with a dry tube. Then, 23 ml (0.24 mol) acetic anhydride was added to the solution and the mixture was stirred vigorously at 65 °C for 24 h. After cooling to room temperature, the product was separated by filtration and washed with diethyl ether three times. Then, the product was placed in a 250 ml conical bottle and 58 ml acetic anhydride was poured into it and the mixture was stirred for 30 min at room temperature in order to purify the DTPAD. The product was separated by vacuum filtration and washed three times with acetic anhydride and diethyl ether. After drying for 24 h at 60 °C, the white product DTPAD was obtained.

**2.3.2 Synthesis of DTPA-functionalized silica gel (SiO<sub>2</sub>-DTPA).** Silica gel was immersed in 6 M HCl at 60 °C for 6 h and washed with distilled water until pH = 7. Then, the treated silica gel was separated by filtration and dried at 60 °C for 12 h. 5 g treated silica gel was dried under vacuum for 3 h at 130 °C and placed in a 100 ml 3-neck flask. Afterward, the amino-functionalized silica gel was prepared by the dropwise addition of 7 ml  $\gamma$ -aminopropyltriethoxysilane (APTES) to 5 g silica gel in 50 ml distilled toluene. Then, the reactants were stirred at 110 °C for 24 h, and collected by filtration, rinsed with acetone and toluene, and finally dried at 70 °C for 24 h. To get DTPA-functionalized silica gel, 2 g amino-functionalized silica gel and 6 g DTPAD were mixed and poured into a 100 ml three-neck flask. Then, 36 ml anhydrous ethanol and 36 ml acetic acid were



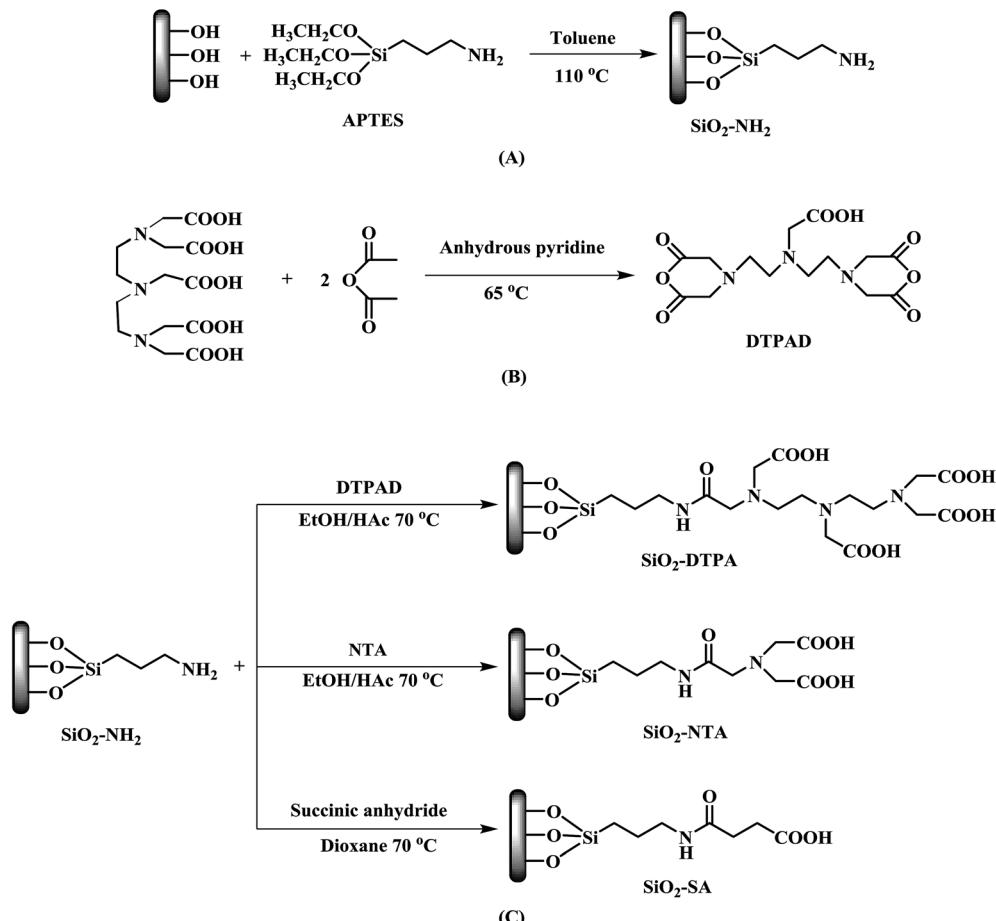


Fig. 1 A schematic illustration of (A)  $\text{SiO}_2\text{-NH}_2$ , (B) DTPAD, (C) polycarboxylic acid functionalized  $\text{SiO}_2$ .

added into the mixture and stirred at 70 °C for 24 h. After cooling to room temperature, the product was separated by filtration and washed with water and acetone and dried at 70 °C for 12 h.<sup>33</sup> The process is illustrated in Fig. 1(C), Step 1.

**2.3.3 Synthesis of  $\text{SiO}_2\text{-DTPA-Pt}$ .** Firstly, 1 g  $\text{H}_2\text{PtCl}_6\cdot 6\text{H}_2\text{O}$  was dissolved in 50 ml *i*-propanol to obtain 0.0386 mol l<sup>-1</sup>  $\text{H}_2\text{PtCl}_6$  solution. Then, 0.8 g  $\text{SiO}_2\text{-DTPA}$  and 80 ml anhydrous ethanol was added into a 100 ml 4-neck flask. Once the heating temperature reached 78 °C, 8 ml *i*-propanol- $\text{H}_2\text{PtCl}_6$  was added to the mixture and further heated to reflux at 78 °C under a continuous nitrogen flow for 9 h. After cooling to room temperature, the yellow product was separated by filtration and washed with ethanol several times. Finally, the product was dried at 60 °C for 24 h. The Pt catalyst was also prepared at different external temperatures (30, 50, 70, 90 and 100 °C) with the corresponding internal temperature being 25, 43, 62, 75 and 78 °C, respectively. The  $\text{SiO}_2\text{-DTPA-Pt}$  was prepared in different solvents including ethanol, *i*-propanol, *n*-butanol and *n*-hexanol at 78 °C.

#### 2.4 Synthesis of Pt catalyst loaded on NTA-functionalized silica gel ( $\text{SiO}_2\text{-NTA-Pt}$ )

To obtain NTA-functionalized silica gel, 10 g NTA and 8 g amino-functionalized silica gel, as prepared in Section 2.3.2,

were mixed and added to a 250 ml three-neck flask. Then, 80 ml anhydrous ethanol and 80 ml acetic acid were poured into the mixture and mechanically stirred at 70 °C for 24 h. After cooling to room temperature, the product was separated by filtration and rinsed with water and acetone and dried at 70 °C for 12 h. The synthetic process is illustrated in Fig. 1(C) Step 2. To get  $\text{SiO}_2\text{-NTA-Pt}$ , 0.4 g  $\text{SiO}_2\text{-NTA}$  and 50 ml anhydrous ethanol were added into a 100 ml 4-neck flask. Once the heating temperature reached 78 °C, 4 ml *i*-propanol- $\text{H}_2\text{PtCl}_6$  (0.0386 mol l<sup>-1</sup>) was added to the mixture and further heated to reflux at 78 °C under a continuous nitrogen flow for 9 h. After cooling to room temperature, the yellow product was separated by filtration and washed with ethanol several times. Finally, the product was dried at 60 °C for 24 h.

#### 2.5 Synthesis of Pt catalyst loaded on SA-functionalized silica gel ( $\text{SiO}_2\text{-SA-Pt}$ )

Fig. 1(C) step 3 shows the preparation process of SA-functionalized silica gel. A total of 6 g butanedioic anhydride, 6 g amino-functionalized silica gel as prepared in Section 2.3.2 and 100 ml dioxane were added into a 250 ml 3-neck flask. The mixture was stirred at 70 °C for 24 h. The product was separated by filtration and rinsed with acetone and water several times. Finally, the SA-functionalized silica gel was dried at 70 °C for

12 h. To obtain  $\text{SiO}_2\text{-SA-Pt}$ , a mixture of 0.6 g  $\text{SiO}_2\text{-SA}$ , 6 ml *i*-propanol- $\text{H}_2\text{PtCl}_6$  solution (0.0386 mol l<sup>-1</sup>) and 60 ml anhydrous ethanol was stirred at 78 °C for 9 h. Then, the product was separated by filtration and washed with ethanol several times and dried at 60 °C for 24 h.

## 2.6 Evaluation and application of the immobilized Pt catalysts

Firstly, 1-hexene hydrosilylation with methyldichlorosilane was used to evaluate the catalytic activities of  $\text{SiO}_2\text{-DTPA-Pt}$ ,  $\text{SiO}_2\text{-NTA-Pt}$  and  $\text{SiO}_2\text{-SA-Pt}$ . The alkane hydrosilylation was tested in a 50 ml conical centrifuge tube which was equipped with a condenser at the top of the tube to avoid evaporation of the solution. Typically, for  $\text{SiO}_2\text{-DTPA-Pt}$ , an appropriate amount of Pt catalyst loaded on DTPA-functionalized silica gel containing  $2.8 \times 10^{-3}$  mmol Pt was added to the 50 ml conical centrifuge tube with a magnetic stirrer. Then, an appropriate amount of 1-hexene (10 mmol) was added to the system and the reactants were stirred at 60 °C for 30 min. Afterward, an appropriate amount of methyldichlorosilane (18 mmol) was added to the system. The reaction mixture was heated to 60 °C and magnetically stirred for 4 h and after cooling down to room temperature, the reaction mixture was separated by centrifugation.  $\text{SiO}_2\text{-NTA-Pt}$  ( $2.3 \times 10^{-3}$  mmol Pt) and  $\text{SiO}_2\text{-SA-Pt}$  ( $2.9 \times 10^{-3}$  mmol Pt) were used to catalyze the model reaction and the experimental conditions and procedures were the same as for the catalytic reaction using  $\text{SiO}_2\text{-DTPA-Pt}$ . The reactants were filtrated with a 0.22 µm microporous filter before quantitative analysis with GC. <sup>1</sup>H NMR spectra were recorded on a Bruker AC-P400 (600 MHz) spectrometer to characterize the structure of the product.

In addition, a series of linear alkenes and ring type alkenes were chosen to evaluate and compare the catalytic activity, selectivity and feasibility of the  $\text{SiO}_2\text{-DTPA-Pt}$ ,  $\text{SiO}_2\text{-NTA-Pt}$  and  $\text{SiO}_2\text{-SA-Pt}$  catalysts. Hydrosilylation reactions between different olefins and methyldichlorosilane were also carried out in a 50 ml conical centrifuge tube which was equipped with a condenser at the top of the tube to avoid evaporation of the solution and a magnetic stirrer. Typical reaction conditions were as follows: 10 mg  $\text{SiO}_2\text{-DTPA-Pt}$  ( $2.8 \times 10^{-3}$  mmol Pt), 15 mg  $\text{SiO}_2\text{-NTA-Pt}$  ( $2.3 \times 10^{-3}$  mmol Pt) or 25 mg  $\text{SiO}_2\text{-SA-Pt}$  ( $2.9 \times 10^{-3}$  mmol Pt) was added to 10 mmol short-chained olefins (1-heptene, 1-octene, styrene, norbornene or cyclohexene), 5.0 mmol olefins (*cis*-hex-2-ene) or 5.0 mmol long-chained alkenes (1-decene, 1-do-decene, 1-tetra-decene, 1-hex-a-decene, or 1-octa-decene). The mixture was stirred at 60 °C for 30 min. Afterward, an appropriate amount of methyldichlorosilane (18 mmol) was added to the mixture. The reactants were heated to 60 °C and magnetically stirred for 5 h for long-chained alkenes or 4 h for other olefins and after cooling down to room temperature, the mixture was separated by centrifugation.

In reusability experiments, 1-hexene hydrosilylation with methyldichlorosilane was used to evaluate the reusability of  $\text{SiO}_2\text{-DTPA-Pt}$ ,  $\text{SiO}_2\text{-NTA-Pt}$  and  $\text{SiO}_2\text{-SA-Pt}$ . After each catalytic reaction for these three Pt catalysts, the reactants could be

separated from the system by centrifugation. Then, the heterogeneous Pt catalysts could be held in the original system and reused for the next catalytic reaction without any other processes.

## 2.7 Characterization of the immobilized Pt catalysts

The intermediates and immobilized platinum catalysts, DTPAD,  $\text{SiO}_2$ ,  $\text{SiO}_2\text{-NH}_2$ ,  $\text{SiO}_2\text{-DTPA}$ ,  $\text{SiO}_2\text{-NTA}$ ,  $\text{SiO}_2\text{-SA}$ ,  $\text{SiO}_2\text{-DTPA-Pt}$ ,  $\text{SiO}_2\text{-NTA-Pt}$  and  $\text{SiO}_2\text{-SA-Pt}$  were characterized using IR. DTPAD was also identified using <sup>1</sup>H NMR. The elemental distributions of the catalysts ( $\text{SiO}_2\text{-DTPA-Pt}$ ,  $\text{SiO}_2\text{-NTA-Pt}$  and  $\text{SiO}_2\text{-SA-Pt}$ ) were analyzed using EDS. The size, morphology and distribution of the catalyst particles were observed using TEM and HRTEM. The samples were prepared by dispersing them in deionized water on a Formvar/carbon film coated Cu grid, followed by drying under ambient conditions. The binding energies of Pt from the catalysts were characterized using XPS. The actual Pt loadings for all the catalysts were determined using AAS. The  $\text{H}_2\text{PtCl}_6$  residual liquid after immobilization was determined using UV spectrometry at wavelengths from 220 nm to 500 nm to investigate the change in valence state of the Pt. The <sup>1</sup>H NMR spectra were recorded on a Bruker AC-P400 (600 MHz) spectrometer to characterize the structure of the products. The yield of the products of the reactions between alkenes and methyldichlorosilane were determined using GC. The GC conditions for short-chained alkenes were as follows: the split ratio was 30 : 1; the sampling volume was 0.8 µl; the column temperature was increased from 60 °C to 260 °C at a rate of 10 °C min<sup>-1</sup>; the time duration for the highest temperature was 5 min; the temperature of injection and detection was 260 °C. The GC conditions of the reactions between long-chained alkenes (1-decene, 1-do-decene, 1-tetra-decene, 1-hex-a-decene, or 1-octa-decene) and methyldichlorosilane were as follows: the column temperature was increased from 60 °C to 280 °C at a rate of 10 °C min<sup>-1</sup>; the duration time for the highest temperature was 5 min; the temperature of injection and detection was 280 °C; the sampling volume was 0.6 µl.

## 3 Results and discussion

### 3.1 Characterization of the catalysts

**3.1.1 IR and NMR analysis of DTPAD.** The IR spectrum of DTPAD is shown in Fig. S1(A).† The absorption bands at 1816 cm<sup>-1</sup> and 1770 cm<sup>-1</sup> can be ascribed to the characteristic bands of anhydride. The absorption at 1641 cm<sup>-1</sup>, 2821 cm<sup>-1</sup> and 2982 cm<sup>-1</sup> originate from the vibration bands of C=O and O-H of the carboxyl group, respectively. In addition, there are absorption bands at 1366 cm<sup>-1</sup>, 1335 cm<sup>-1</sup> and 1111 cm<sup>-1</sup>, corresponding to the vibration absorption of the C-N group, and the peaks at 1298–1204 cm<sup>-1</sup> are related to C-O stretching.<sup>34</sup> <sup>1</sup>H NMR (DMSO, 600 MHz) is shown in Fig. S1(B)† and these NMR data are consistent with the characteristic peaks of DTPAD.<sup>35</sup>

**3.1.2 IR analysis of the Pt catalysts.** Comparisons of the FT-IR spectra of  $\text{SiO}_2$ ,  $\text{SiO}_2\text{-NH}_2$ ,  $\text{SiO}_2\text{-DTPA}$ ,  $\text{SiO}_2\text{-NTA}$ ,  $\text{SiO}_2\text{-SA}$ ,  $\text{SiO}_2\text{-DTPA-Pt}$ ,  $\text{SiO}_2\text{-NTA-Pt}$  and  $\text{SiO}_2\text{-SA-Pt}$  are shown in



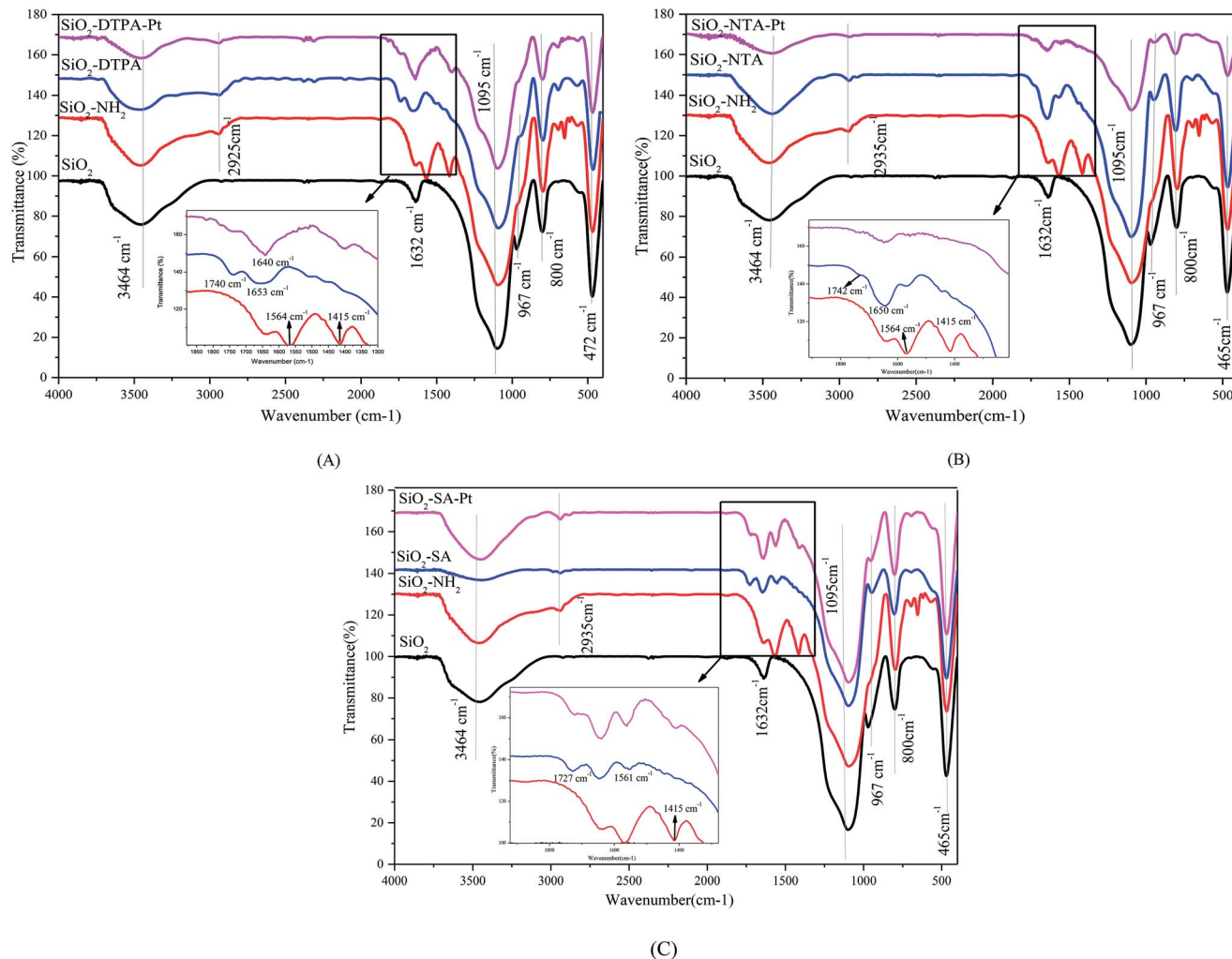


Fig. 2 IR spectra of (A) silica gel,  $\text{SiO}_2\text{-NH}_2$ ,  $\text{SiO}_2\text{-DTPA}$  and  $\text{SiO}_2\text{-DTPA-Pt}$ , (B) silica gel,  $\text{SiO}_2\text{-NH}_2$ ,  $\text{SiO}_2\text{-NTA}$  and  $\text{SiO}_2\text{-NTA-Pt}$  and (C)  $\text{SiO}_2\text{-NH}_2$ ,  $\text{SiO}_2\text{-SA}$  and  $\text{SiO}_2\text{-SA-Pt}$ .

Fig. 2(A–C). In the  $\text{SiO}_2$  spectrum, the large, broad and intense bands at  $1095\text{ cm}^{-1}$  and  $800\text{ cm}^{-1}$  correspond to  $\text{Si}-\text{O}-\text{Si}$  stretching, the peak at  $472\text{ cm}^{-1}$  corresponds to  $\text{Si}-\text{O}-\text{Si}$  bending and the peak at  $967\text{ cm}^{-1}$  arises from  $\text{Si}-\text{OH}$  bending (observed in all samples). Another two peaks at  $1632\text{ cm}^{-1}$  and  $3464\text{ cm}^{-1}$  correspond to isolated hydroxyl groups on the silica surface.<sup>36</sup> In the  $\text{SiO}_2\text{-NH}_2$  spectrum, new peaks appear at  $2925\text{ cm}^{-1}$  and  $1415\text{ cm}^{-1}$  corresponding to  $-\text{CH}_2-$  stretching and bending vibrations of the pendant propyl chain and the band at  $1564\text{ cm}^{-1}$  is from  $-\text{NH}_2-$  vibrations.<sup>14</sup> For  $\text{SiO}_2\text{-DTPA}$ ,  $\text{SiO}_2\text{-NTA}$ , and  $\text{SiO}_2\text{-SA}$ , the two peaks at  $1740\text{ cm}^{-1}$  and  $1653\text{ cm}^{-1}$  ( $\text{SiO}_2\text{-DTPA}$ ),  $1742\text{ cm}^{-1}$  and  $1650\text{ cm}^{-1}$  for  $\text{SiO}_2\text{-NTA}$  and  $1727\text{ cm}^{-1}$  and  $1647\text{ cm}^{-1}$  for  $\text{SiO}_2\text{-SA}$  are from carbonyl groups. The disappearance of carbonyl groups at  $1740\text{ cm}^{-1}$  in  $\text{SiO}_2\text{-DTPA-Pt}$ ,  $1742\text{ cm}^{-1}$  in  $\text{SiO}_2\text{-NTA-Pt}$  and  $1727\text{ cm}^{-1}$  in  $\text{SiO}_2\text{-SA-Pt}$  indicates that Pt successfully anchors to the modified silica gel through carbonyl groups.

**3.1.3 TEM and EDS analysis of the Pt catalysts.** The TEM images of  $\text{SiO}_2\text{-DTPA-Pt}$ ,  $\text{SiO}_2\text{-NTA-Pt}$  and  $\text{SiO}_2\text{-SA-Pt}$  are presented in Fig. 3(A–C), where the dark spots on the surface of the

catalysts could be Pt and the morphology and distribution of Pt could be observed. Characteristic patterns of Pt (111) planes ( $d = 0.227\text{ nm}$ ) were also observed. Highly dispersed Pt particles were detected in the TEM images of  $\text{SiO}_2\text{-DTPA-Pt}$  and the size of the Pt particles was about 3–4 nm, and they had better dispersion than in  $\text{SiO}_2\text{-NTA-Pt}$  and  $\text{SiO}_2\text{-SA-Pt}$ . Some aggregated particles larger than 5 nm were detected in the TEM images of  $\text{SiO}_2\text{-NTA-Pt}$  and  $\text{SiO}_2\text{-SA-Pt}$ . These results indicate that the DTPA functionalized silica could be used as an efficient support for forming highly dispersed, ultra small sized Pt particles. As shown in Fig. 3(D–F), the EDS analysis revealed the presence of Pt and the corresponding elements of C, O, N, Si and Cl in all of the catalysts ( $\text{SiO}_2\text{-DTPA-Pt}$ ,  $\text{SiO}_2\text{-NTA-Pt}$  and  $\text{SiO}_2\text{-SA-Pt}$ ). Before the EDS determination, the samples need to be coated on the Cu grid of a formavar/carbon film. This is the reason for Cu in the X-ray spectra.

**3.1.4 Analysis of Pt valence states for the Pt catalysts.** To explore the valence state change of Pt on immobilization on  $\text{SiO}_2\text{-DTPA}$ ,  $\text{SiO}_2\text{-NTA}$  and  $\text{SiO}_2\text{-SA}$ , the residual  $\text{H}_2\text{PtCl}_6$  solutions were analyzed using UV and the data are shown in

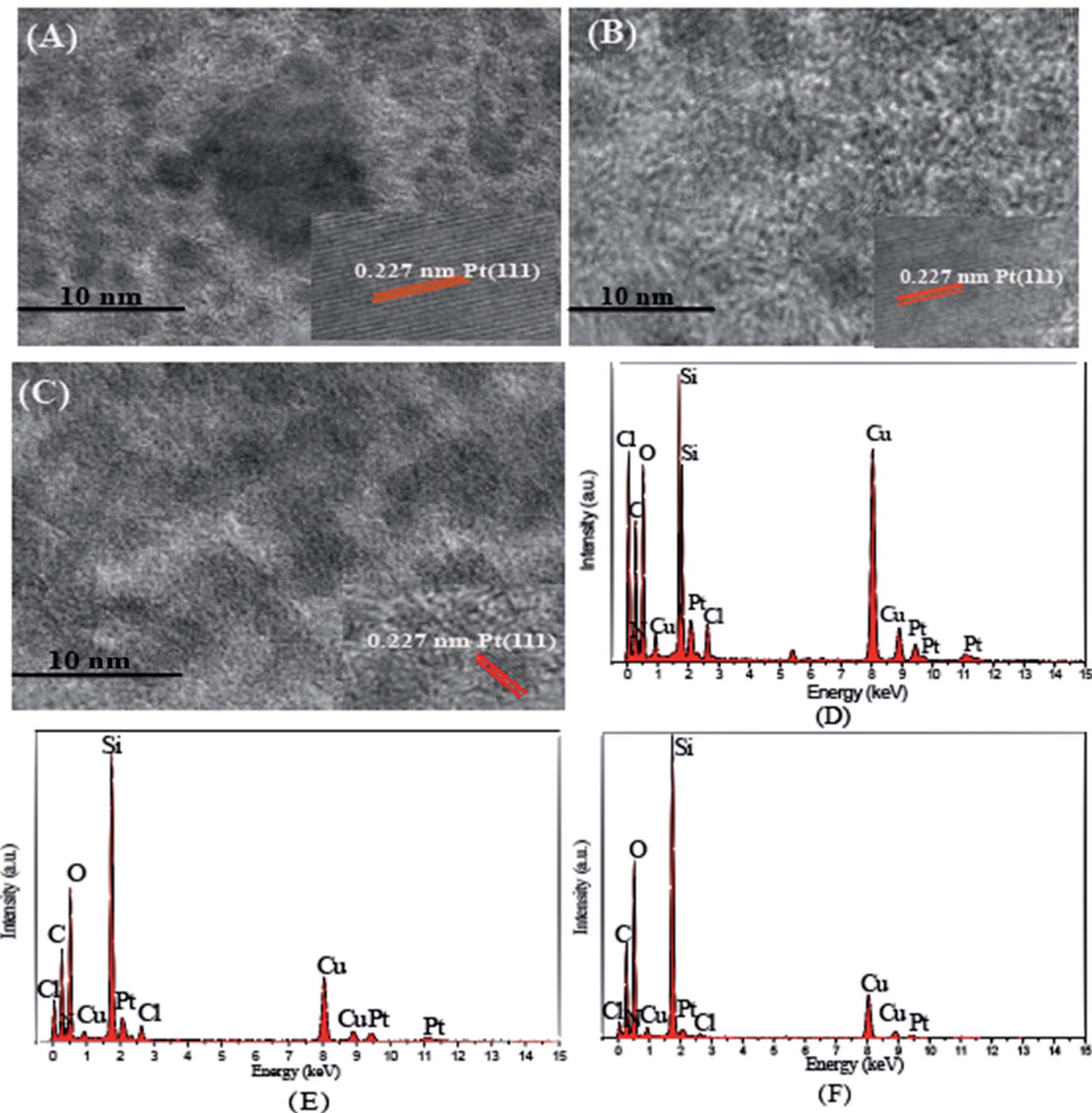


Fig. 3 The TEM images of (A)  $\text{SiO}_2$ -DTPA-Pt, (B)  $\text{SiO}_2$ -NTA-Pt and (C)  $\text{SiO}_2$ -SA-Pt; the EDS spectra of (D)  $\text{SiO}_2$ -DTPA-Pt, (E)  $\text{SiO}_2$ -NTA-Pt, and (F)  $\text{SiO}_2$ -SA-Pt.

Fig. S2(A-D).<sup>†</sup> The results indicate that their maximum absorbance was quite different from the primary absorbance. The absorbance of the original  $\text{H}_2\text{PtCl}_6$  solution appears at 265 nm (Fig. S2(A)<sup>†</sup>) and is consistent with the absorbance of Pt(iv) reported before.<sup>37</sup> The absorbance at 265 nm for the residual Pt decreased to 243 nm for  $\text{SiO}_2$ -DTPA-Pt and  $\text{SiO}_2$ -NTA-Pt (Fig. S2(B and C)<sup>†</sup>) and decreased to 242 nm for  $\text{SiO}_2$ -SA-Pt (Fig. S2(D)<sup>†</sup>), which is consistent with the absorbance of Pt particles reported before.<sup>21</sup> The changes confirm that Pt has been successfully immobilized on the APCA-functionalized silica gel with other forms.

**3.1.5 XPS and AAS analysis of the Pt catalysts.** XPS was employed to obtain surface information on Pt oxidation states and compositions of the  $\text{SiO}_2$ -DTPA-Pt,  $\text{SiO}_2$ -NTA-Pt, and  $\text{SiO}_2$ -SA-Pt catalysts. As shown in Fig. 4 (A), the spectra also indicate the presence of O, C, N, Si, Cl and Pt for  $\text{SiO}_2$ -DTPA-Pt,  $\text{SiO}_2$ -NTA-Pt, and  $\text{SiO}_2$ -SA-Pt, which is in agreement with the EDS data. The results of the elemental analysis of these three Pt catalysts are shown in Table 1. The C content was 32.6%, 30.4% and 24.6%, while the N content was 5.6%, 4.2% and 3.6% for  $\text{SiO}_2$ -DTPA-Pt,  $\text{SiO}_2$ -NTA-Pt, and  $\text{SiO}_2$ -SA-Pt respectively. Fig. 4(B-D) shows the Pt 4f spectra of  $\text{SiO}_2$ -DTPA-Pt,  $\text{SiO}_2$ -NTA-Pt

and  $\text{SiO}_2$ -SA-Pt. Deconvolution of the Pt 4f region shows the presence of two pairs of doublets. The most intense doublet with binding energies of 71.6 (Pt 4f<sub>7/2</sub>) and 74.8 eV (Pt 4f<sub>5/2</sub>) was attributed to metallic Pt.<sup>38</sup> Peaks at 72.9 (Pt 4f<sub>7/2</sub>) and 76.4 eV (Pt 4f<sub>5/2</sub>) could be assigned to Pt<sup>δ+</sup>. The amount of metallic Pt was 63.6% in  $\text{SiO}_2$ -DTPA-Pt, which was higher than that of  $\text{SiO}_2$ -NTA-Pt (59.8%) and  $\text{SiO}_2$ -SA-Pt (54.9). These results could be attributed to the fact that DTPA has a stronger charge binding ability than NTA or SA<sup>39</sup> and more C and N exists in DTPA functionalized silica. The formation of metallic Pt might be caused by the interaction of the polycarboxylic acid with Pt.<sup>40</sup>

The actual Pt loadings for the polycarboxylic acid-functionalized silica supported Pt catalysts were determined using AAS. The data shows that the Pt loading for  $\text{SiO}_2$ -DTPA-Pt was 0.287 mmol g<sup>-1</sup> or 5.59 wt%, which was higher than that of

Table 1 Elemental analysis of Pt catalysts by XPS

Catalyst	Mass concentration (%)				Relative atomic percentage (%)	
	C 1s	N 1s	O 1s	Pt 4f	Metallic Pt	Pt <sup>δ+</sup>
$\text{SiO}_2$ -DTPA-Pt	32.6	5.6	41.6	1	63.64	36.36
$\text{SiO}_2$ -NTA-Pt	30.4	4.2	44.4	0.9	59.83	40.17
$\text{SiO}_2$ -SA-Pt	24.6	3.6	50.5	0.5	54.86	45.14

3.84 wt% for  $\text{SiO}_2$ -EDTA-Pt,<sup>31</sup> 2.93 wt% for  $\text{SiO}_2$ -NTA-Pt, and 2.30 wt% for  $\text{SiO}_2$ -SA-Pt. The amount of Pt in these APCA-functionalized silica supported Pt catalysts follows the order:  $\text{SiO}_2$ -DTPA-Pt >  $\text{SiO}_2$ -EDTA-Pt >  $\text{SiO}_2$ -NTA-Pt >  $\text{SiO}_2$ -SA-Pt. These

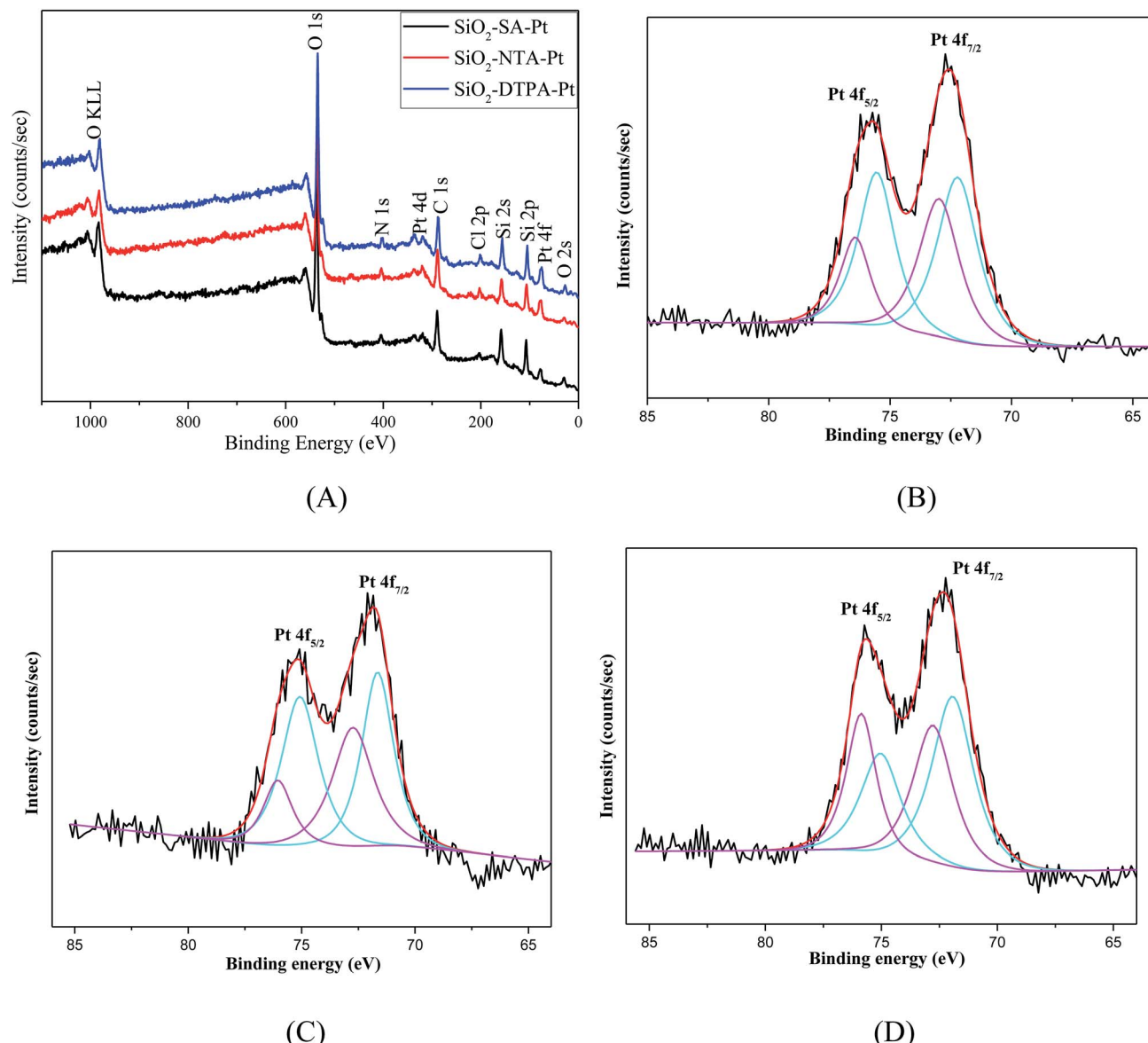


Fig. 4 XPS spectra of  $\text{SiO}_2$ -DTPA-Pt,  $\text{SiO}_2$ -NTA-Pt, and  $\text{SiO}_2$ -SA-Pt (A), XPS Pt 4f spectra of  $\text{SiO}_2$ -DTPA-Pt (B),  $\text{SiO}_2$ -NTA-Pt (C), and  $\text{SiO}_2$ -SA-Pt (D).

results indicate that DTPA could help to immobilize more Pt on the modified silica gel.

### 3.2 Catalytic properties of the Pt catalysts

**3.2.1 Catalytic activity of immobilized Pt catalysts.** Herein, 1-hexene hydrosilylation with methyldichlorosilane was used to evaluate the catalytic properties of  $\text{SiO}_2$ -DTPA-Pt,  $\text{SiO}_2$ -NTA-Pt and  $\text{SiO}_2$ -SA-Pt (all of these catalysts were prepared at 80 °C in anhydrous ethanol). The results are shown in Fig. S5† and Table 2. In the GC chromatograms shown in Fig. S5A,† only one product peak around 11.92 min was observed and its retention time is consistent with that of 1-dichloromethylhexylsilane. The data of its  $^1\text{H-NMR}$  spectrum (see Fig. S5B†) verified that the reaction product was dichloromethylhexylsilane and that the three immobilized Pt catalysts have good selectivity for the hydrosilylation of 1-hexene and methyldichlorosilane.  $\text{SiO}_2$ -DTPA-Pt showed the highest activity, achieving the desired product in a 99.6% yield with a 1.79  $\text{s}^{-1}$  TOF, and  $\text{SiO}_2$ -NTA-Pt also showed high activity, achieving 1-hexyl-methyl-dichlorosilane in a 94.4% yield with a 1.27  $\text{s}^{-1}$  TOF. Meanwhile, the yield of 1-hexyl-methyl-dichlorosilane catalyzed by  $\text{SiO}_2$ -SA-Pt was 97.1% with a lower TOF (0.14  $\text{s}^{-1}$ ). This data indicates that the three immobilized Pt catalysts have high activity for the hydrosilylation of 1-hexene and methyldichlorosilane under optimal conditions. However, the variation trend of these three catalysts represented by the TOF was different.  $\text{SiO}_2$ -SA-Pt showed the lowest TOF with a product yield that was only 33.8% after a 2 h reaction while the yield of dichloromethylhexylsilane was 95.9% for  $\text{SiO}_2$ -DTPA-Pt or 88.8% for  $\text{SiO}_2$ -NTA-Pt. These results demonstrate that the constituent of the polycarboxylic acid group plays a critical role in the hydrosilylation of 1-hexene and methyldichlorosilane.

**3.2.2 Optimization and evaluation of the preparation conditions for  $\text{SiO}_2$ -DTPA-Pt.** The catalytic activity of EDTA-functionalized silica supported Pt or  $\text{Al}_2\text{O}_3$ -supported Pt catalysts could be strongly affected by their preparation conditions.<sup>18,31</sup> Therefore, the influence of the preparation conditions (temperature and solvents) were investigated for  $\text{SiO}_2$ -DTPA-Pt.

The Pt catalyst was prepared as in Section 2.3.3 at different external temperatures (30, 50, 70, 90 or 100 °C) with the corresponding internal temperatures being 25, 43, 62, 75 and 78 °C, respectively. The results (Table 3) reveal that the preparation temperature has a vital influence on the catalytic activity of  $\text{SiO}_2$ -DTPA-Pt. The yield of the product increased and the

inductive period shortened with increasing preparation temperature for  $\text{SiO}_2$ -DTPA-Pt. When the preparation temperature was lower than the boiling point of ethanol (78 °C), the Pt loading on  $\text{SiO}_2$ -DTPA-Pt increased from 0.128 mmol  $\text{g}^{-1}$  to 0.231 mmol  $\text{g}^{-1}$  as the temperature increased, and the yield increased from 88.0% to 95.3% after 4 h. Meanwhile, the yield increased to the maximum (99.6%) as the preparation temperature increased to 78 °C (0.287 mmol  $\text{g}^{-1}$  Pt). Therefore, it could be concluded that Pt(iv) was able to be present as the stable and active Pt species when the preparation temperature was increased to 78 °C. This hypothesis is consistent with the UV/Vis spectra of the residual Pt solutions of  $\text{SiO}_2$ -DTPA-Pt prepared at different internal temperatures in ethanol. As shown in Fig. S3,† it could be observed that the absorbance at 265 nm gradually decreased and the absorbance at 243 nm appeared as the preparation temperature increased from 25 °C to 78 °C. As we can see from Section 3.1.4, the absorbance of Pt(iv) at 265 nm was consistent with that of samples prepared at 25 °C, while the absorbance at 243 nm for the Pt prepared at 78 °C was consistent with the absorbance of Pt particles reported before.<sup>21</sup> These results indicate that the catalytic activity is dependent on the preparation temperature; when the temperature increases to 78 °C, the yield increases to the maximum, which might be caused by the conversion of Pt(iv) to Pt particles.

The effect of preparation solvents including ethanol, *i*-propanol, *n*-butanol and *n*-hexanol on the catalytic activity was investigated. As in Section 2.3.3, we prepared  $\text{SiO}_2$ -DTPA-Pt at 78 °C using different solvents. The results (Table 4) suggest that the catalytic activity for  $\text{SiO}_2$ -DTPA-Pt is largely related to the synthetic solvents. It was revealed that catalysts prepared in three other solvents had low catalytic activities (39.1%, 46.0% and 8.5% in *i*-propanol, *n*-butanol and *n*-hexanol respectively) while the yield was 99.6% using ethanol as the immobilized solvent. As shown in Fig. S4,† the UV/Vis spectra of the residual Pt solutions for  $\text{SiO}_2$ -DTPA-Pt prepared with different solvents indicate that the absorbance of Pt at 243 nm using ethanol as the solvent was consistent with the absorbance of Pt particles reported before.<sup>21</sup> Meanwhile, the absorbance was still at 265 nm when using *n*-butanol as the preparation solvent, which indicated that the Pt was immobilized on the  $\text{SiO}_2$ -DTPA in the form of Pt(iv). The absorbance of Pt increased to 277 nm when the preparation solvent was *n*-hexanol and disappeared when using *i*-propanol as the solvent which indicated that the Pt

Table 2 Comparison of the hydrosilylation activities of immobilized Pt catalysts

Catalyst	Platinum content (mmol $\text{g}^{-1}$ )	Yield (%) <sup>a</sup>						TOF <sup>b</sup> ( $\text{s}^{-1}$ )
		0.5 h	1 h	2 h	3 h	4 h		
$\text{SiO}_2$ -DTPA-Pt	0.287	90.3	94.3	95.9	99.1	99.6	1.79	
$\text{SiO}_2$ -NTA-Pt	0.150	52.5	87.2	88.8	90.2	94.4	1.27	
$\text{SiO}_2$ -SA-Pt	0.118	7.5	17.7	33.8	80.3	97.1	0.14	

<sup>a</sup> Conditions: Pt amount:  $\text{SiO}_2$ -DTPA-Pt:  $2.8 \times 10^{-3}$  mmol Pt,  $\text{SiO}_2$ -NTA-Pt:  $2.3 \times 10^{-3}$  mmol Pt,  $\text{SiO}_2$ -SA-Pt:  $2.9 \times 10^{-3}$  mmol Pt; temperature: 60 °C; adding order: silane is added to alkene. <sup>b</sup> Turnover frequency measured at 0.5 h.



Table 3 Effect of the preparation temperature on catalytic activity of  $\text{SiO}_2$ -DTPA-Pt

Catalyst	Yield (%) <sup>a</sup>							TOF <sup>b</sup> (s <sup>-1</sup> )
	External temperature (°C)	Internal temperature (°C)	Platinum content (mmol g <sup>-1</sup> )	0.5 h	1.0 h	2.0 h	3.0 h	
30	25	0.128	7.5	14.3	56.0	71.5	88.0	0.15
50	43	0.133	11.8	22.3	73.4	88.3	89.4	0.23
70	62	0.195	27.6	69.7	74.7	83.1	91.2	0.55
90	75	0.231	68.8	83.9	87.7	92.7	95.3	1.37
100	78	0.287	90.3	94.3	95.9	99.1	99.6	1.79

<sup>a</sup> Conditions: Pt amount:  $\text{SiO}_2$ -DTPA-Pt:  $2.8 \times 10^{-3}$  mmol Pt; temperature: 60 °C; adding order: silane is added to alkene. <sup>b</sup> Turnover frequency measured at 0.5 h.

might be connected with DTPA functionalized silica in other forms. The solvents could affect the catalytic activity by influencing the valence state of Pt. In this case, ethanol was chosen as the optimal solvent for immobilizing Pt on the polycarboxylic acid-functionalized silica gel.

**3.2.3 Effect of catalytic conditions on the immobilized Pt catalysts.** Herein, we tried to find optimized catalytic conditions for alkane hydrosilylation catalyzed by the three Pt catalysts. In this case, the following conditions were investigated: the amount of the heterogeneous Pt catalyst, the reaction temperature, the reaction time, the adding order of the reactants and the ratio of reactants.

The alkene hydrosilylation activity with methyldichlorosilane catalyzed by immobilized Pt catalysts exhibited a strong dependence on temperature. Higher temperatures could give higher activity with a shorter time.<sup>41</sup> The influence of the temperature (40–80 °C) on the catalytic activity of the polycarboxylic acid-functionalized silica supported Pt catalysts at different times was inspected. Fig. 5(A and B) show the yield of the products, dichloromethylhexylsilane, catalyzed by  $\text{SiO}_2$ -DTPA-Pt and  $\text{SiO}_2$ -NTA-Pt at different temperatures.  $\text{SiO}_2$ -DTPA-Pt showed the highest activity, achieving the desired product in 99.6% yield with a 1.79 s<sup>-1</sup> TOF at 60 °C, and  $\text{SiO}_2$ -NTA-Pt also showed high activity, achieving 1-hexyl-methyl-dichlorosilane in 94.4% yield with a 1.27 s<sup>-1</sup> TOF. When the temperature was below or over 60 °C, the TOF of both  $\text{SiO}_2$ -DTPA-Pt and  $\text{SiO}_2$ -NTA-Pt was lower than that at 60 °C, with values of 0.25, 0.63, 1.07 and 0.95 at 40 °C, 50 °C, 70 °C and 80 °C, respectively, for

$\text{SiO}_2$ -DTPA-Pt. Meanwhile, for  $\text{SiO}_2$ -NTA-Pt, the TOF was 0.11, 0.24, 0.93 and 0.95 at 40 °C, 50 °C, 70 °C and 80 °C, respectively. In this case, 60 °C gave the best result of all the temperatures evaluated (40 °C to 80 °C), and temperature plays a significant role in the catalytic activity of the polycarboxylic acid-functionalized Pt catalysts.

In order to get a higher yield for 1-hexene hydrosilylation with methyldichlorosilane, a series of reaction times of 0.5 h, 1 h, 2 h, 3 h, and 4 h were investigated. As shown in Table 2, it is clearly observed that the yield of the products reached the maximum after 4 h (99.6% for  $\text{SiO}_2$ -DTPA-Pt and 94.4% for  $\text{SiO}_2$ -NTA-Pt). The yield was 90.3% after the first 0.5 h, and increased slowly to 94.3% (1 h), then reached 99.6% after 4 h for  $\text{SiO}_2$ -DTPA-Pt. In contrast, for  $\text{SiO}_2$ -NTA-Pt, the yield was 52.5% after 0.5 h and increased rapidly to 87.2% from 0.5 h to 1 h and increased slowly after 1 h, then reached the maximum of 94.4% after 4 h. These results indicate that the reaction time plays an important role in the catalytic activity of the immobilized Pt catalysts, and 4 h was chosen as the reaction time for the experiments.

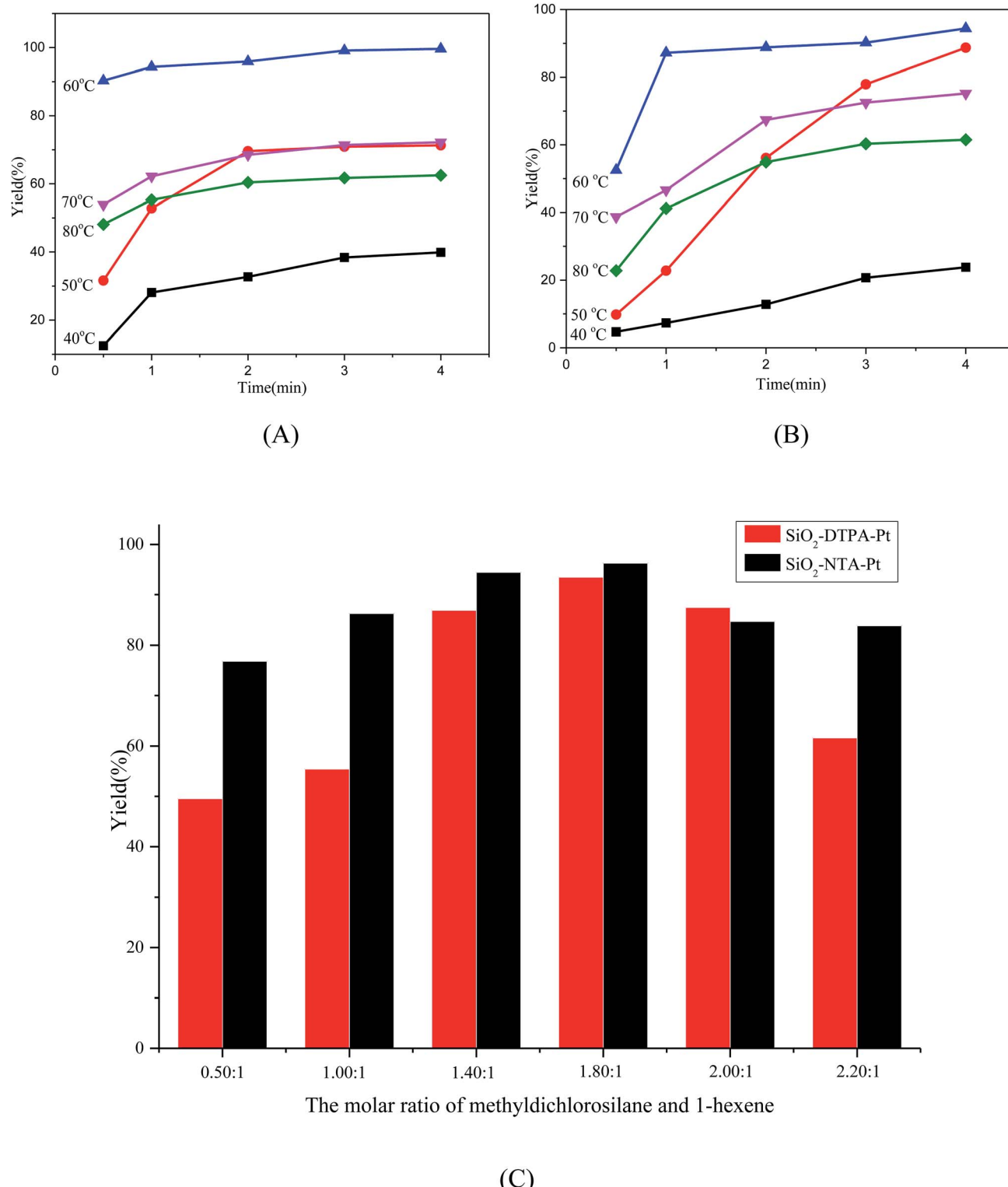
Hydrosilylable olefins are resistant to insertion into the Pt-Si bond and not to hydrosilylation if no excess silane is present.<sup>42</sup> Bearing this in mind, the effect of the ratio between the two reactants (methyldichlorosilane and 1-hexene) was inspected for  $\text{SiO}_2$ -DTPA-Pt and  $\text{SiO}_2$ -NTA-Pt, with ratios of 0.50 : 1, 1.00 : 1, 1.40 : 1, 1.80 : 1, 2.00 : 1, and 2.20 : 1. The data shown in Fig. 5(C) reveal that when the ratio of the reactants was 0.50 : 1, the yield was the lowest (49.52%) for  $\text{SiO}_2$ -DTPA-Pt

Table 4 Effect of the preparation solvent on the catalytic activity of  $\text{SiO}_2$ -DTPA-Pt

Catalyst	Yield (%) <sup>a</sup>							TOF <sup>b</sup> (s <sup>-1</sup> )
	Platinum content (mmol g <sup>-1</sup> )	0.5 h	1 h	2 h	3 h	4 h		
Solvent of preparation								
Ethanol	0.287	90.3	94.3	95.9	99.1	99.6	1.79	
<i>i</i> -Propanol	0.195	4.0	17.8	21.5	28.6	39.1	0.080	
<i>n</i> -Butanol	0.231	4.9	5.0	15.5	41.2	46.0	0.098	
<i>n</i> -Hexanol	0.199	1.0	4.3	7.7	8.3	8.5	0.022	

<sup>a</sup> Conditions: Pt amount:  $\text{SiO}_2$ -DTPA-Pt:  $2.8 \times 10^{-3}$  mmol Pt; temperature: 60 °C; adding order: silane is added to alkene. <sup>b</sup> Turnover frequency measured at 0.5 h.





**Fig. 5** The yield of the product (%) vs. temperature (°C) at different times for 1-hexane hydrosilylation with methyldichlorosilane catalyzed by  $\text{SiO}_2\text{-DTPA-Pt}$  (A) and  $\text{SiO}_2\text{-NTA-Pt}$  (B). The yield (%) vs. reactant ratio for 1-hexane hydrosilylation with methyldichlorosilane catalyzed by  $\text{SiO}_2\text{-DTPA-Pt}$  and  $\text{SiO}_2\text{-NTA-Pt}$  (C). Conditions: (A and B) Pt amount:  $\text{SiO}_2\text{-DTPA-Pt}$ :  $2.8 \times 10^{-3}$  mmol Pt,  $\text{SiO}_2\text{-NTA-Pt}$ :  $2.3 \times 10^{-3}$  mmol Pt; time: 0.5 h, 1 h, 2 h, 3 h and 4 h; temperature: 40, 50, 60, 70 and 80 °C; adding order: silane is added to the alkene. (C) The ratios of silane and alkene were 0.50 : 1, 1.00 : 1, 1.40 : 1, 1.80 : 1, 2.00 : 1 and 2.20 : 1.

because of the residual 1-hexane. The yield of the dichloromethylhexylsilane increased from 55.41% to 93.45% as the ratio rose from 1.00 : 1 to 1.80 : 1. When the ratio continually increased, the yields of the product dropped from 87.49% to 81.62%. Meanwhile for  $\text{SiO}_2$ -NTA-Pt, the variation trend was similar to that for  $\text{SiO}_2$ -DTPA-Pt, and it had the highest activity when the ratio was 1.80 : 1. Therefore, we used the ratio of 1.80 : 1 for the alkene hydrosilylation.

Results from the experiments with  $\text{SiO}_2$ -DTPA-Pt or  $\text{SiO}_2$ -NTA-Pt and those previously described<sup>31</sup> for  $\text{SiO}_2$ -EDTA-Pt showed that the hydrosilylation conditions such as reaction time, reaction temperature, and the ratio of reactants were similar for the APCA-functionalized silica supported Pt catalysts. In view of this, the reaction conditions for  $\text{SiO}_2$ -SA-Pt were the same as those for  $\text{SiO}_2$ -DTPA-Pt and  $\text{SiO}_2$ -NTA-Pt except for the catalyst dosage and the additive sequence of reactants.

The amount of the heterogeneous Pt catalyst plays a vital role in the catalytic activity. Therefore, the effect of the amount of the Pt catalyst on alkene hydrosilylation was inspected for these three immobilized Pt catalysts. The results revealed that the maximum yield reached 99.8%, 98.5% and 97.1% respectively for  $\text{SiO}_2$ -DTPA-Pt ( $2.8 \times 10^{-3}$  mmol Pt),  $\text{SiO}_2$ -NTA-Pt ( $2.3 \times 10^{-3}$  mmol Pt) and  $\text{SiO}_2$ -SA-Pt ( $2.9 \times 10^{-3}$  mmol Pt). The variation trend of these respective catalytic activities affected by catalytic dosage was similar for these three catalysts. When catalysts were used that contained less Pt, *i.e.*,  $1.4 \times 10^{-3}$  mmol for  $\text{SiO}_2$ -DTPA-Pt (37.0%),  $7.5 \times 10^{-4}$  mmol for  $\text{SiO}_2$ -NTA-Pt (62.4%) and  $1.18 \times 10^{-3}$  mmol for  $\text{SiO}_2$ -SA-Pt (32.8%), the yields were lower. These results indicate that the yields of the products of alkene hydrosilylation catalyzed by the polycarboxylic acid functionalized silica supported Pt catalysts were strongly dependent on the amount of heterogeneous Pt catalyst. A lower amount of Pt catalyst may lead to more by-products and limit the catalytic activity of the immobilized Pt catalysts.

The Chalk-Harrod mechanism was firstly proposed for alkene hydrosilylation catalyzed by Pt catalyst.<sup>43</sup> For the mechanism, the alkene was coordinated to the center of Pt to form an alkene-Pt complex, then, the silane was introduced to the alkene-Pt complex for oxidative addition. The coordinated olefin was inserted into the Pt-H bond and the hydrosilylation product was eliminated by reduction. The step of inserting the olefin into the Pt-H bond is rate-limiting in alkene hydrosilylation.<sup>44</sup> Thus, the adding order of the reactants might have an effect on the hydrosilylation. In this case, the influence of the adding order of the reactants on the alkene hydrosilylation for these three immobilized Pt catalysts was inspected. As shown in Fig. 6, it was clearly revealed that the catalytic activity of the model reaction was largely dependent on the adding order of the reactants. The varied trends of the yields of reactions catalyzed by these three Pt catalysts were similar; when methyldichlorosilane was poured into the reaction after 1-hexene and the Pt catalyst were stirred for 30 min, the yields of dichloromethylhexylsilane increased to 97.14%, 94.42% and 95.45% for  $\text{SiO}_2$ -DTPA-Pt,  $\text{SiO}_2$ -NTA-Pt and  $\text{SiO}_2$ -SA-Pt, respectively. Meanwhile, the yields decreased to 82.5%, 90.0% and 66.6%

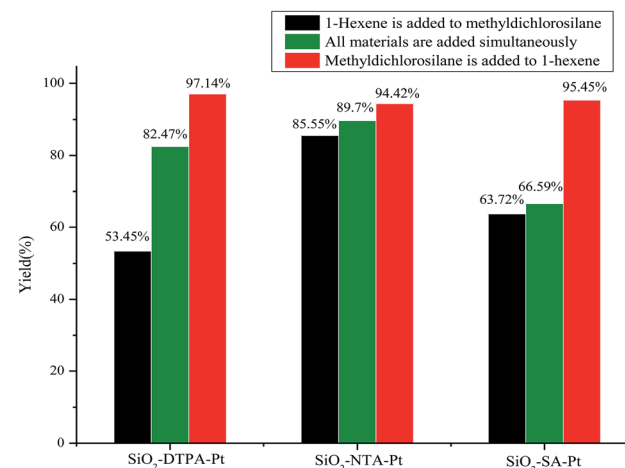


Fig. 6 Effect of the adding order of reactants on the yield of product for  $\text{SiO}_2$ -DTPA-Pt,  $\text{SiO}_2$ -NTA-Pt and  $\text{SiO}_2$ -SA-Pt. Conditions: Pt amount:  $\text{SiO}_2$ -DTPA-Pt:  $2.8 \times 10^{-3}$  mmol Pt,  $\text{SiO}_2$ -NTA-Pt:  $2.3 \times 10^{-3}$  mmol Pt,  $\text{SiO}_2$ -SA-Pt:  $2.9 \times 10^{-3}$  mmol Pt. Adding order: silane is added to alkene, all reactants are added simultaneously, alkene is added to silane.

when the reactants were added to the system at the same time and the yields reduced to 53.5%, 85.6% and 63.7% when 1-hexene was poured into the reaction after methyldichlorosilane and the Pt catalyst were stirred for 30 min. These results indicate that the adding order of the reactants is a predominant influence in alkene hydrosilylation. A plausible catalytic mechanism for polycarboxylic acid-functionalized Pt catalysts is shown in Fig. 7. The mixture of Pt catalyst and alkene at a certain temperature can activate the double bond, and form the alkene-Pt complex. The olefin could then be inserted into the Pt-H bond more easily and could improve the catalytic activity of the Pt catalyst.

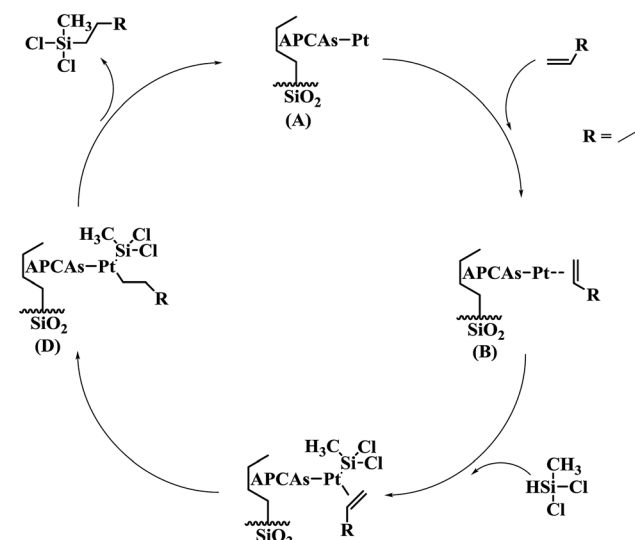


Fig. 7 A plausible catalytic mechanism for the polycarboxylic acid-functionalized Pt catalysts.



### 3.3 The applicability of $\text{SiO}_2$ -DTPA-Pt, $\text{SiO}_2$ -NTA-Pt and $\text{SiO}_2$ -SA-Pt

As shown in Fig. 8, an array of substituted linear and ring type alkenes were used to investigate the applicability of the polycarboxylic acid-functionalized silica supported Pt catalysts. The catalytic products were analyzed using  $^1\text{H}$  NMR.

The product of reactions using 1-heptene is dichloromethylheptylsilane, whose  $^1\text{H}$  NMR spectrum is shown in Fig. S6A.<sup>†</sup> The conversion of 1-heptene catalyzed by  $\text{SiO}_2$ -DTPA-Pt,  $\text{SiO}_2$ -NTA-Pt and  $\text{SiO}_2$ -SA-Pt was 98.9%, 98.8% and 97.9%, respectively, and the selectivity was 99%, 99% and 99%, respectively, which is better than the selectivity of homogeneous platinum catalyst (94%). The  $^1\text{H}$  NMR spectrum of the product for 1-octene is shown in Fig. S6B<sup>†</sup> and agreed with that of standard dichloromethyloctylsilane. The conversion of 1-octene catalyzed by  $\text{SiO}_2$ -DTPA-Pt,  $\text{SiO}_2$ -NTA-Pt and  $\text{SiO}_2$ -SA-Pt was 98.6%, 98.1% and 97.0%, respectively, and the selectivity was 99%, 99% and 99%, respectively, which is better than the selectivity of homogeneous platinum catalyst (95%). The product of 1-decene was dichlorodecylmethylsilane, and the  $^1\text{H}$  NMR spectrum is shown in Fig. S6C.<sup>†</sup> The conversion of 1-decene catalyzed by  $\text{SiO}_2$ -DTPA-Pt,  $\text{SiO}_2$ -NTA-Pt and  $\text{SiO}_2$ -SA-Pt was 97.8%, 97.7% and 97.1%, respectively, and the selectivity was 99%, 99% and 99%, respectively, which is better than the selectivity of homogeneous platinum catalyst (95%). The product of 1-dodecene was dichlorododecylmethylsilane, whose  $^1\text{H}$  NMR spectrum is shown in Fig. S6D.<sup>†</sup> The conversion of 1-dodecene catalyzed by  $\text{SiO}_2$ -DTPA-Pt,  $\text{SiO}_2$ -NTA-Pt and  $\text{SiO}_2$ -SA-Pt was 97.8%, 97.7% and 97.1%, respectively, and the selectivity was 99%, 98% and 99%, respectively, which is better than the selectivity of homogeneous platinum catalyst (95%). The product of 1-tetradecylene was dichloromethyltetradecylsilane, whose  $^1\text{H}$  NMR spectrum is shown in Fig. S6E.<sup>†</sup> The conversion of 1-tetradecylene catalyzed by  $\text{SiO}_2$ -DTPA-Pt,  $\text{SiO}_2$ -NTA-Pt and  $\text{SiO}_2$ -SA-Pt was 98.1%, 92.3% and 93.2%, respectively, and the selectivity was 99%, 99% and 99%, respectively, which is better than the selectivity of homogeneous platinum catalyst (95%). The  $^1\text{H}$  NMR spectrum of the product for 1-hexadecene is shown in Fig. S6F.<sup>†</sup> The conversion of 1-hexadecene catalyzed by  $\text{SiO}_2$ -DTPA-Pt,  $\text{SiO}_2$ -NTA-Pt and  $\text{SiO}_2$ -SA-Pt was 95.0%, 93.4% and 94.0%, respectively, and the selectivity was 99%, 98% and 97%, respectively, which is better than the selectivity of homogeneous

platinum catalyst (94%). The product of 1-octadecene was dichloromethyloctadecylsilane, whose  $^1\text{H}$  NMR spectrum is shown in Fig. S6G.<sup>†</sup> The conversion of 1-octadecene catalyzed by  $\text{SiO}_2$ -DTPA-Pt,  $\text{SiO}_2$ -NTA-Pt and  $\text{SiO}_2$ -SA-Pt was 95.0%, 93.4% and 94.0%, respectively, and the selectivity was 99%, 99% and 99%, respectively, which is apparently better than the selectivity of homogeneous platinum catalyst (87%). The product of styrene is dichloromethylphenethylsilane, whose  $^1\text{H}$  NMR spectrum is shown in Fig. S6H.<sup>†</sup><sup>45</sup> The conversion of styrene catalyzed by  $\text{SiO}_2$ -DTPA-Pt,  $\text{SiO}_2$ -NTA-Pt and  $\text{SiO}_2$ -SA-Pt was 95.5%, 98.8% and 95.7%, respectively, and the selectivity was 99%, 99% and 99%, respectively, which is apparently better than the selectivity of homogeneous platinum catalyst (63%).

The above data suggest that these three immobilized Pt catalysts could also catalyze the hydrosilylation of other linear alkenes effectively. Linear terminal olefins gave very good yields of the corresponding silylated products (Table 5, entries 1 to 8) and had high selectivity.

Little attention has been paid to the hydrosilylation of internal double bonds so far, which are generally known to be far less reactive toward hydrosilylation than terminal olefins.<sup>46</sup> But for our research, we tried to use the immobilized platinum catalysts to catalyze the hydrosilylation of internal double bonds and chose *cis*-hex-2-ene as a model compound. In GC, the product, dichloromethylhexylsilane, appeared at 12.724 min, which was separated well from *cis*-hex-2-ene at 3.001 min. High conversion was achieved using an internal olefin (Table 5, entry 9 for *cis*-hex-2-ene); the conversion of the internal olefin was 95.2%, 92.7% and 92.3% for *cis*-hex-2-ene catalyzed by  $\text{SiO}_2$ -DTPA-Pt,  $\text{SiO}_2$ -NTA-Pt and  $\text{SiO}_2$ -SA-Pt, respectively, which was superior to the 33% achieved by Karstedt's catalyst.<sup>44</sup> High selectivities were also observed (99%, 99% and 99%, respectively). These results indicate that these three immobilized Pt catalysts may potentially be used in the hydrosilylation reaction of internal olefins.

Norbornene and cyclohexene were used to test the catalytic activity of these three immobilized Pt catalysts for ring type alkenes. In GC, the products could be separated well from norbornene or cyclohexene. The conversion of cyclohexene catalyzed by  $\text{SiO}_2$ -DTPA-Pt,  $\text{SiO}_2$ -NTA-Pt and  $\text{SiO}_2$ -SA-Pt was 30.4%, 22.0% and 22.4%, respectively. However, cyclohexene was unable to undergo hydrosilylation catalyzed by Karstedt's catalyst.<sup>44</sup> These results indicate that these three immobilized Pt catalysts are superior to homogeneous Pt catalysts for the hydrosilylation of cyclohexene and methyldichlorosilane. In contrast, high conversion (92.5%, 90.0% and 88.6% catalyzed by  $\text{SiO}_2$ -DTPA-Pt,  $\text{SiO}_2$ -NTA-Pt and  $\text{SiO}_2$ -SA-Pt, respectively) and selectivity (100%) were obtained for norbornene. The  $^1\text{H}$  NMR spectrum of the product is shown in Fig. S6I.<sup>†</sup> These results reveal that these three immobilized Pt catalysts were more active for the hydrosilylation of norbornene than that of cyclohexene. It appears that the substitution pattern at the  $\alpha$ -C or the possible agostic interaction of the bridging methylene protons of norbornene might exert a beneficial effect. The forced boat conformation of norbornene confers it with a higher reactivity than the chair conformation of cyclohexene.

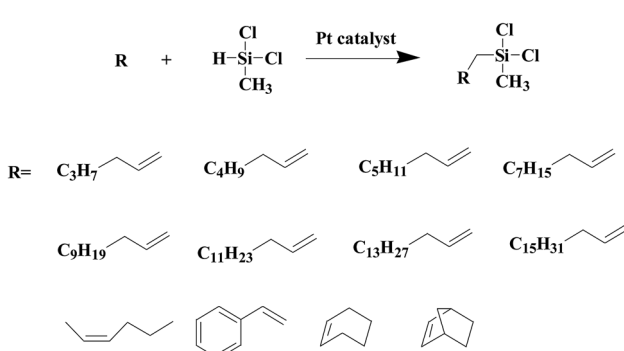


Fig. 8 The substrate scope of the hydrosilylation reaction.



Table 5 Hydrosilylation of selected substrates

Entry	Catalyst	Substrate	Product <sup>c</sup>	Yield (%) <sup>a</sup>	Selectivity <sup>b</sup>
1	SiO <sub>2</sub> -DTPA-Pt			98.9	99%
	SiO <sub>2</sub> -NTA-Pt			98.8	99%
	SiO <sub>2</sub> -SA-Pt			97.9	99%
2	SiO <sub>2</sub> -DTPA-Pt			98.6	99%
	SiO <sub>2</sub> -NTA-Pt			98.1	99%
	SiO <sub>2</sub> -SA-Pt			97.0	99%
3	SiO <sub>2</sub> -DTPA-Pt			97.8	99%
	SiO <sub>2</sub> -NTA-Pt			97.7	99%
	SiO <sub>2</sub> -SA-Pt			97.1	99%
4	SiO <sub>2</sub> -DTPA-Pt			97.3	99%
	SiO <sub>2</sub> -NTA-Pt			95.1	98%
	SiO <sub>2</sub> -SA-Pt			90.8	99%
5	SiO <sub>2</sub> -DTPA-Pt			98.1	99%
	SiO <sub>2</sub> -NTA-Pt			92.3	99%
	SiO <sub>2</sub> -SA-Pt			93.2	99%
6	SiO <sub>2</sub> -DTPA-Pt			95.0	97%
	SiO <sub>2</sub> -NTA-Pt			93.4	98%
	SiO <sub>2</sub> -SA-Pt			94.0	97%
7	SiO <sub>2</sub> -DTPA-Pt			93.5	99%
	SiO <sub>2</sub> -NTA-Pt			93.1	99%
	SiO <sub>2</sub> -SA-Pt			91.6	99%
8	SiO <sub>2</sub> -DTPA-Pt			95.5	99%
	SiO <sub>2</sub> -NTA-Pt			98.8	99%
	SiO <sub>2</sub> -SA-Pt			95.7	99%
9	SiO <sub>2</sub> -DTPA-Pt			95.2	99%
	SiO <sub>2</sub> -NTA-Pt			92.7	99%
	SiO <sub>2</sub> -SA-Pt			92.3	99%
10	SiO <sub>2</sub> -DTPA-Pt			92.5	100%
	SiO <sub>2</sub> -NTA-Pt			90.0	100%
	SiO <sub>2</sub> -SA-Pt			88.6	100%
11	SiO <sub>2</sub> -DTPA-Pt			30.4	100%
	SiO <sub>2</sub> -NTA-Pt			22.0	100%
	SiO <sub>2</sub> -SA-Pt			22.4	100%

<sup>a</sup> Conditions: Pt amount: SiO<sub>2</sub>-DTPA-Pt:  $2.8 \times 10^{-3}$  mmol Pt, SiO<sub>2</sub>-NTA-Pt:  $2.3 \times 10^{-3}$  mmol Pt, SiO<sub>2</sub>-SA-Pt:  $2.9 \times 10^{-3}$  mmol Pt; temperature: 60 °C; time: 4 h; adding order: silane is added to alkene. <sup>b</sup> Selectivity was determined using GC. <sup>c</sup> Products were determined using <sup>1</sup>H NMR. Please see Fig. S4 for the relevant NMR spectra.

### 3.4 The reusability of SiO<sub>2</sub>-DTPA-Pt, SiO<sub>2</sub>-NTA-Pt and SiO<sub>2</sub>-SA-Pt

To investigate the reusability of polycarboxylic acid-functionalized silica supported Pt catalysts, 1-hexene hydrosilylation with methyl dichlorosilane was used to do the recycling experiments. After each catalytic reaction for these three Pt catalysts, the reactants could be separated by centrifuging them from the system. Then, the heterogeneous Pt catalysts could be held in the original system and reused in the next catalytic reaction without any processing. As shown in Fig. 9, the results reveal that SiO<sub>2</sub>-DTPA-Pt shows a very good activity over thirteen catalytic runs with a small loss in the yield of 1-hexyl-

methyl dichlorosilane (80% after thirteen catalytic runs). Meanwhile, SiO<sub>2</sub>-NTA-Pt could be reused seven times and the yield of the final run was 82%. However, the yield of 1-hexyl-methyl dichlorosilane drastically dropped over the three runs (96.9%, 62.8% and 30.9%) for SiO<sub>2</sub>-SA-Pt. It was found in leaching experiments that the Pt content of SiO<sub>2</sub>-DTPA-Pt decreased from 5.59 wt% to 5.28 wt% after being reused 4 times, which indicates that the loss of Pt occurs during the reaction. The Pt content decreased to 4.94 wt%, 4.43 wt% and 3.86 wt% after being reused 7, 10 and 13 times, respectively. In other words, the average loss of Pt was approximately 1.44 ppm in each reaction, which was lower than the active concentration



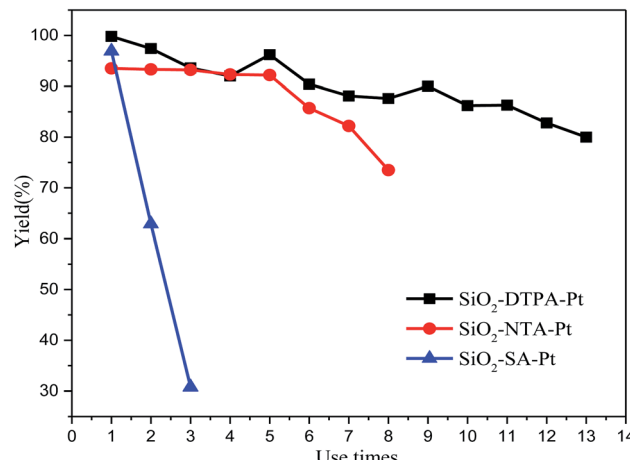


Fig. 9 Reuse cycles of SiO<sub>2</sub>-DTPA-Pt, SiO<sub>2</sub>-NTA-Pt and SiO<sub>2</sub>-SA-Pt.

(i.e. 10 ppm) for homogeneous Pt catalysts. The loss of the Pt catalyst in each run was an important reason contributing to the decrease in the yield. However, the difference in the binding abilities of DTPA, NTA and SA may cause the difference in the reusability for these three immobilized Pt catalysts. DTPA had much stronger interactions with Pt than NTA and SA, and had little decrease in activity after repeated use.

## 4 Conclusions

A series of novel polycarboxylic acid-functionalized silica supported Pt catalysts was successfully synthesized in our work. The XPS results indicated the existence of charge transfer from Pt to the coordination atoms of DTPA, NTA and SA. These three new immobilized Pt catalysts were shown to have wide applications, high activity, selectivity and reusability for alkene hydrosilylation. Among them, SiO<sub>2</sub>-DTPA-Pt showed the best catalytic ability and could be reused 13 times with less loss of yield of the product because of the strong connections of DTPA with Pt. The three new polycarboxylic acid-functionalized Pt catalysts may potentially be used in industrial alkene hydrosilylation.

## Conflicts of interest

There are no conflicts to declare.

## Abbreviations

DTPA	Diethylenetriaminepentaacetic acid
DTPAD	Diethylenetriaminepentaacetic dianhydride
EDTA	Ethylenediaminetetraacetic acid
NTA	Nitrilotriacetic acid
SA	Succinic acid
AAS	Atomic absorption spectroscopy
IR	Infrared spectroscopy
NMR	Nuclear magnetic resonance
UV	Ultraviolet spectroscopy

TEM	Transmission electron micrographs
HRTEM	High resolution transmission electron micrographs
GC	Gas chromatography
EDS	Energy dispersive X-ray spectrometer
XPS	X-ray photoelectron spectroscopic
APTES	γ-aminopropyltriethoxysilane
SiO <sub>2</sub> -DTPA	DTPA-functionalized silica gel
SiO <sub>2</sub> -DTPA-Pt	SiO <sub>2</sub> -DTPA supported Pt
Pt	
SiO <sub>2</sub> -NTA	NTA-functionalized silica gel
SiO <sub>2</sub> -NTA-Pt	SiO <sub>2</sub> -NTA supported Pt
SiO <sub>2</sub> -SA	SA-functionalized silica gel
SiO <sub>2</sub> -SA-Pt	SiO <sub>2</sub> -SA supported Pt
TOF	turnover frequency

## Acknowledgements

The authors are grateful for support from the National Natural Science Foundation of China (No. 21605112) and the Youth Fund of the Science and Technology Committee of Tianjin Municipal Government (No. 15JCQNJC43200).

## Notes and references

- 1 J. L. Speier, *Adv. Organomet. Chem.*, 1979, **17**, 407–447.
- 2 M. Shelef, J. H. Jones, J. T. Kummer, K. Otto and E. E. Weaver, *Environ. Sci. Technol.*, 1971, **5**(9), 790–798.
- 3 M. Itoh, K. Motoki, M. Saito, J. Iwamoto and M. Ken-Ichi, *Bull. Chem. Soc. Jpn.*, 2009, **82**(9), 1197–1202.
- 4 F. Y. Zhao, Y. Ikushima and M. Arai, *J. Catal.*, 2004, **224**(2), 479–483.
- 5 C. Exner, A. Pfaltz, M. Studer and H. U. Blaser, *Adv. Synth. Catal.*, 2003, **345**(11), 1253–1260.
- 6 M. A. Yoichi, T. Arakawa, H. Hocke and Y. Uozumi, *Angew. Chem., Int. Ed.*, 2007, **119**, 718–720.
- 7 J. Li, N. Wang, Z. H. Ma, Z. H. Hu and L. Y. Sun, *Rare Met. Mater. Eng.*, 2013, **42**(2), 259–262.
- 8 J. S. Rhee, R. M. Sneeringer and A. S. Penzias, *Coord. Chem. Rev.*, 2011, **255**(13), 1440–1459.
- 9 J. C. Stephen, *Silicon*, 2009, **1**, 57–58.
- 10 B. Karstedt, *US Pat.* 3814730, 1973.
- 11 I. E. Markó, S. Stérin, O. Buisine, G. Mignani, P. Branlard, B. Tinan and J. P. Declercq, *Science*, 2002, **298**(5591), 204–206.
- 12 M. Poyatos, F. A. Maisse, B. L. Stephane and L. H. Gade, *Organometallics*, 2006, **25**(10), 2634–2641.
- 13 K. Kaneda, K. Ebitani, T. Mizugaki and K. Mori, *J. Cheminform.*, 2006, **79**, 781–1016.
- 14 J. Li, C. H. Yang, L. Zhang and T. L. Ma, *J. Organomet. Chem.*, 2011, **696**(9), 1845–1849.
- 15 Y. Bai, J. Peng, J. Y. Li, G. Q. Lai and X. N. Li, *Curr. Catal.*, 2012, **1**, 180–185.
- 16 G. D. Thomas, R. Sayah, M. L. Zanota, S. Marrot, L. Veyre, C. Thieuleux and V. Meille, *Chem. Commun.*, 2017, **53**(20), 2962–2965.



17 X. J. Cui, K. Junge, X. C. Dai, C. Kreyenschulte, M. P. Martina, W. Sebastian, F. Shi, B. Angelika and B. Matthias, *ACS Cent. Sci.*, 2017, **3**(6), 580–585.

18 Y. Fort, A. Silvestri and H. Graindorge, *J. Mol. Catal. A: Chem.*, 1996, **112**(2), 311–316.

19 H. T. Yang, Z. P. Fang, X. Y. Fu and L. F. Tong, *Catal. Commun.*, 2008, **9**(6), 1092–1095.

20 A. Kowalewska, *J. Organomet. Chem.*, 2008, **693**(12), 2193–2199.

21 Y. Bai, S. F. Zhang, Y. Deng, J. J. Peng, J. Y. Li, Y. Q. Hu and X. N. Li, *J. Colloid Interface Sci.*, 2013, **394**(1), 428–433.

22 Z. M. Michalska, K. Strzelec and J. W. Sobczak, *J. Mol. Catal. A: Chem.*, 2000, **156**(1), 91–102.

23 M. Chauhan, B. J. Hauck, L. P. Keller and P. Boudjouk, *J. Organomet. Chem.*, 2002, **645**, 1–13.

24 F. Y. Rao, S. J. Deng, C. Chen and N. Zhang, *Catal. Commun.*, 2014, **46**(5), 1–5.

25 A. Francisco, R. Buitrago, Y. Moglie, R. M. Javier, S. E. Antonio and Y. Miguel, *J. Organomet. Chem.*, 2011, **696**(1), 368–372.

26 B. Nowack, *Environ. Sci. Technol.*, 2002, **36**(19), 4009–4016.

27 S. D. N. Almeida and H. E. Toma, *Hydrometallurgy*, 2016, **161**, 22–28.

28 Y. Shiraishi, G. Nishimura, H. Takayuki and I. Komasa, *Ind. Eng. Chem. Res.*, 2002, **41**(20), 5065–5070.

29 A. Baraka, P. J. Hall and M. J. Heslop, *J. Hazard. Mater.*, 2007, **140**(1–2), 86–94.

30 O. Ikodiyi, M. Uzoamaka and I. Ezeani, *International Journal of Innovative Research and Development*, 2017, **6**, 117–127.

31 F. T. Li and Y. X. Li, *J. Mol. Catal. A: Chem.*, 2016, **420**, 254–263.

32 M. Tülü and K. E. Geckeler, *Polym. Int.*, 1999, **48**, 909–914.

33 A. H. Mark and R. Edward, *Sep. Sci. Technol.*, 2007, **42**(2), 261–283.

34 K. Nakamoto, *Sexually Transmitted Infections*, 2008, **85**(3), 182–186.

35 J. Greiser, T. Hagemann, T. Niksch, P. Traber, S. Kupfer, S. Gräfe, H. Görts, W. Weigand and M. Freesmeyer, *Eur. J. Inorg. Chem.*, 2015, **24**, 4125–4137.

36 Y. Q. An, M. Chen, Q. Xue and W. M. Liu, *J. Colloid Interface Sci.*, 2007, **311**(2), 507–513.

37 M. Luty-Blocho, M. Wojnicki, K. Paclawski and K. Fitzner, *Chem. Eng. J.*, 2013, **226**, 46–51.

38 R. F. Nie, D. Liang, L. Shen, J. Gao, P. Chen and Z. Y. Hou, *Appl. Catal., B*, 2012, **127**, 212–220.

39 C. Zhang, T. Wang, X. Liu and Y. J. Ding, *J. Mol. Catal. A: Chem.*, 2016, **424**, 91–97.

40 C. Liu, G. Li, D. R. Kauffman, G. S. Pang and R. C. Jin, *J. Colloid Interface Sci.*, 2014, **423**(423), 123–128.

41 R. H. Hu, L. F. Zha and M. Z. Cai, *Catal. Commun.*, 2010, **11**, 563–566.

42 A. K. Roy and R. B. Taylor, *J. Am. Chem. Soc.*, 2002, **124**(32), 9510–9524.

43 A. J. Chalk and J. F. Harrod, *J. Am. Chem. Soc.*, 1965, **87**(1), 583–597.

44 T. K. Meister, K. Riener, P. Gigler, J. Stohrer, W. A. Herrmann and E. K. Fritz, *ACS Catal.*, 2016, **6**(2), 1274–1284.

45 B. J. Brisdon and A. M. Watts, *J. Chem. Soc., Dalton Trans.*, 1985, **10**(10), 2191–2194.

46 J. S. Rhee, R. M. Sneeringer and A. S. Penzias, *Coord. Chem. Rev.*, 2011, **255**(13), 1440–1459.

